Applied Catalysis B: Environmental 134–135 (2013) 34–45

Contents lists available at SciVerse ScienceDirect

Applied Catalysis B: Environmental

journal homepage: www.elsevier.com/locate/apcatb

Nickel cerium olivine catalyst for catalytic gasification of biomass

Singfoong Cheah[a,*], Katherine R. Gaston[a], Yves O. Parent[a], Mark W. Jarvis[a], Todd B. Vinzant[b], Kristin M. Smith[a], Nicholas E. Thornburg[a], Mark R. Nimlos[a], Kimberly A. Magrini-Bair[a]

[a] National Bioenergy Center, National Renewable Energy Laboratory, 1617 Cole Blvd., Golden, CO 80401, USA
[b] Chemical and Biochemical Center, National Renewable Energy Laboratory, 1617 Cole Blvd., Golden, CO 80401, USA

ARTICLE INFO

Article history:
Received 1 September 2012
Received in revised form
23 November 2012
Accepted 17 December 2012
Available online 25 December 2012

Keywords:
Gasification
Tar
Olivine
Chemical looping
Syngas
Tar reforming
Pyrolysis
Biomass gasification
Biofuel

ABSTRACT

A nickel cerium modified olivine was used as a fluidized bed material in a biomass gasifier and the impact of the modification on biomass conversion, product gas composition, and tar speciation at different temperatures of oak gasification was measured. The experiments were conducted in the pyrolysis mode, without additional input of steam or oxygen (e.g., from air) into the system. In both plain and modified olivine, carbon- and hydrogen-based yields in light gases produced increased as temperature increased from 600 to 800 °C. Using modified olivine resulted in significant improvement in carbon- and hydrogen-based yields and substantial reduction in tars and methane. With modified olivine, the biochar produced at 800 °C was 40% less than that with plain olivine. Characterization of the fresh and post-reaction catalyst showed that a fraction of the NiO was reduced in situ in the gasifier by the syngas. In addition, the catalyst was also contributing oxygen to the environment inside the gasifier in a chemical-looping like mode, resulting in less char and coke formation than that of gasification of biomass without an additional oxygen source. Statistical analysis of molecular beam mass spectrometry data provided detailed tar speciation information under different gasification conditions. At both 650 and 800 °C, the modified olivine was effective in producing more syngas either through conversion of hydrocarbon rich tars into syngas or blocking the pathway for hydrocarbon rich tar formation. However, the impact of the modified olivine in converting oxygenates (that are primarily derived from deconstruction of biomass) into deoxygenated compounds was probably minimal.

1. Introduction

To reduce green house gas emissions and to ensure a source of long-term, reliable renewable transportation fuels, there is great interest in developing economical and efficient biomass to biofuel technologies. Gasification of biomass to syngas is a promising route, as the syngas can be used to produce liquid biofuels through Fisher–Tropsch synthesis [1,2]; to produce dimethyl ether (DME) [3] which can be used as a diesel substitute; or to produce alcohol and advanced biofuels through microbial conversion [4]. During gasification, secondary reactions can produce tars, components that condense at 400–500 °C, resulting in problematic downstream processing as well as loss of carbon efficiency (since the production of tar corresponds to a decrease in CO production, a major component of syngas) [5,6]. There has been extensive research on catalytic tar removal downstream of the gasifier [7–12] and the approach has been found effective and ready for commercial pilot testing.

Though less frequently investigated, several literature reports have indicated that catalytic gasification can significantly reduce or eliminate tar content in the product gas generated from biomass gasification [13–18]. García et al. studied the catalytic pyrolysis (no steam added) and gasification (steam or CO_2 added) of biomass using co-precipitated nickel aluminate catalysts at 650–850 °C [13,19–23]. For catalytic pyrolysis at 650 °C, most of the replicates show gas phase carbon yields in the 50–60% range [20], depending on the catalyst to biomass ratio, the calcination temperature of the catalyst, and whether the catalyst was reduced in situ [20,22]. Increasing the temperature to 700 °C in their catalytic pyrolysis experiments did not significantly impact the gas phase carbon yield [21]. At 700 °C with steam added, the gas phase carbon yield averages 80% for all the runs reported, with the yield closer to 100% for the earlier runs [13]. Garcia et al. concluded that at 700 °C, the addition of steam to the gasification process increases H_2 and CO_2 production primarily through the effect of the catalyst on the water gas shift reaction [13].

The Zaragoza group and another research group at the University of Twente [17,24] further conducted extensive research on the gasification of pyrolysis oil. The two-stage pyro-gasification process offers additional process control and inorganic reduction but does

* Corresponding author. Tel.: +1 303 384 7707; fax: +1 303 384 6363.
E-mail address: Singfoong.cheah@nrel.gov (S. Cheah).

0926-3373/$ – see front matter © 2012 Elsevier B.V. All rights reserved.
http://dx.doi.org/10.1016/j.apcatb.2012.12.022

require both a pyrolyzer and a gasifier in the biomass conversion process.

Several research groups have reported that iron in olivine, a mineral often used as the fluidizing material in biomass gasifiers, may have catalytic activity. They also endeavored to modify olivine to impart further catalytic activities to the material. Some of the modified olivines were tested for gas phase reforming reactions (no biomass present) while others were tested for catalytic gasification with biomass. Courson et al. impregnated olivine with nickel and tested the catalysts for dry and steam reforming of methane [25,26]. Swierczynski et al. conducted extensive characterization of olivine and nickel-impregnated olivine and used methane and toluene as model compounds to investigate the tar-reforming activity of the modified catalyst [15,27]. The Gas Technology Institute and Ohio State University conducted a detailed study of the impact of thermal vs. aqueous impregnations on the structure and property of several different types of nickel modified olivine and the use of the modified olivine for tar reforming and catalytic gasification [28,29]. To improve the attrition resistance of the catalytic material further, researchers at the Gas Technology Institute also investigated the synthesis and use of glass–ceramics that incorporates NiO as an active component [30,31] as a tar-reforming catalyst.

Rapagna et al. enriched olivine with 10 wt.% iron and reported that steam gasification of biomass with the Fe-enriched olivine reduced tar content by 60% and improved gas yield by 40% [32]. Recently, Virginie et al. used Fe-enriched olivine for biomass gasification in a dual fluidized bed, i.e., the catalyst is cycled between a combustor and a gasifier [18]. They concluded that the Fe-olivine can act as a catalyst for tar and hydrocarbon reforming, as well as an oxygen carrier that transfers oxygen from the combustor to the gasifier, with part of the oxygen used to burn volatile compounds.

In addition to catalytic gasification, Dauenhauer et al. used a rhodium catalyst operating in a combination of partial oxidation and flash volatilization mode to convert biomass into gas [33]. The gas stream produced consists of H_2, CO, CO_2, and light hydrocarbons. The carbon selectivity was quantified, with approximately 65% selectivity for CO_2 and 29% selectivity for CO.

Corella et al. compared the use of olivine and dolomite as fluidized bed material [34,35] and quantified the relative merits of using dolomite in a downstream reactor (downstream-dolomite) vs. in the gasifier itself (in-bed dolomite) [36]. By comparing gas and tar yields of the two different configurations, they concluded that "down-stream-dolomite" only confers slight advantage than "in-bed-dolomite". They hypothesized that the contact between gas-phase tar molecules and dolomite is better in a "downstream-dolomite" configuration because there are no char and biomass particles in a downstream reactor, though they also concluded that a second bed of dolomite is not necessary if the gasifier bed is well designed and operated. The authors also hypothesized that the observed relatively high tar reduction efficiency of "in-bed dolomite" compared to "downstream dolomite" may be due to "nascent tars" in the gasifier that are less refractory than the types of tars in secondary reactor [36]. Detailed tar composition analysis in both the gasifier and downstream reactor would be useful to test the hypothesis.

In a number of studies the quantity of tar was determined by mass balance (difference between raw biomass and the sum of light gas and char formed) or impinger sampling. Speciation of the type of tars via impinge sampling has to be conducted off-line, e.g., collection of the tars followed by GC–MS analysis [18]. Rapagna et al. used a HPLC/UV method to study tar composition [32]. The HPLC/UV method has been used extensively for identification and quantification of polycyclic aromatic hydrocarbons.

Molecular-beam mass spectrometry (MBMS) is a method that allows universal detection of a large number of species from biomass pyrolysis and gasification, including oxygenates, linear hydrocarbons, and polycyclic aromatic hydrocarbons (PAHs). The advantage of this method is that the hot gases flow over the sampling orifice, creating an expansion at the outlet that is nearly adiabatic and isentropic. This yields effective quenching of further chemical reactions of the gas stream before it passes through a skimmer to generate a molecular beam. This beam is ionized with a relatively low energy (22.5 eV) electron beam to minimize fragmentation of the sampled products. Details of the species detected via pyrolysis and tar species determination using MBMS are reported in the literature [37–40]. The use of MBMS for measurement of gases released during catalytic gasification thus allows us to determine the type of tar species present under different experimental conditions. The detailed data on the types of tar molecules present can be incorporated into detailed modeling of the chemical kinetics inside the gasifier and can also useful in catalytic mechanism investigation.

In this work, we build upon the previous research, but pursue a new catalyst composition, and several new data collection and analysis methods to advance the state of the art in this area and to elucidate new information. For this research we used a nickel-cerium-based catalyst without preliminary reduction; we conducted the gasification experiments in a 4″ fluidized bed reactor with on-line MBMS analysis to speciate syngas tars; and used statistical analyses to quantify the impact of the catalyst on tars and oxygenate molecules. We interpreted the gas and char yield data using thermodynamic modeling of the gas composition and evaluated the potential impact of the material both as a catalyst and an oxygen source that reduces coke formation in the system.

Table 1
Composition of white oak used in catalytic gasification experiments.

Loss on drying (wt.%)	5.28
Elemental analysis (wt.%, dry and ash free)	
C	50.1
O	43.3
H	5.5
N	0.3
S	0.2
Ash (wt.%, dry)	0.5

2. Experimental

2.1. Material synthesis and material properties determination

The white oak feedstock used in this work was sieved to 18–40 mesh (sieve sizes 1.0 mm and 0.42 mm) fractions, with the average particle size being 0.7 mm. The composition of the white oak is shown in Table 1. The olivine used in the gasifier and used for the catalyst preparation was supplied by AGSCO. Inductively coupled plasma analysis of the olivine indicates that there is 4.4% Fe and 0.25% Ni in the as-received material. The particle size distribution of the olivine is 80–1000 μm, as determined with a Mastersizer 2000 particle size analyzer (Malvern Instruments). Water was used as a dispersant in the measurements using a Hydro 2000G accessory for the particle analyzer.

A nickel-cerium on olivine catalyst was synthesized for this research using incipient wetness impregnation. The catalyst was prepared by drop-wise addition of a solution saturated in nickel and cerium nitrate to an olivine support. The salts used in the aqueous solution preparation are nickel (II) nitrate hexahydrate ($Ni(NO_3)_2{\cdot}6H_2O$, CAS # 13478-00-7, Alfa Aesar stock number 12222) and cerium (III) nitrate hexahydrate ($Ce(NO_3)_3{\cdot}6H_2O$, CAS # 10294-41-4, Alfa Aesar stock # 11329). A saturated solution of nickel and cerium nitrate was prepared by dissolving 250 g $Ni(NO_3)_2{\cdot}6H_2O$ and 38.8 g $Ce(NO_3)_3{\cdot}6H_2O$ in water that was kept at 80 °C, with the final solution volume being 200 ml. The prepared

catalyst was dried at 110 °C for greater than 12 h in a vacuum-oven then calcined at 450 °C for 1 h followed by calcination at 800 °C for 4 h in air. The ramp rate from room temperature to 450 °C and 450 °C to 800 °C is 3 °C/min. The prepared catalyst contained 2 wt.% Ni and 0.5 wt.% Ce. The BET surface areas of the fresh and post-gasification catalysts were measured via Kr adsorption at liquid nitrogen temperature using a Quantachrome Quadrasorb SI instrument. Prior to BET measurements, outgassing of the material was conducted under vacuum at a temperature of 300 °C.

2.2. Catalyst performance using the 4″ fluidized bed reactor research gasifier

Catalytic gasification experiments were conducted using an indirectly heated 4″ diameter fluidized bed research gasifier. Dry nitrogen was used as a fluidizing gas and the average gas residence time in the gasifier was 5 s. More detailed descriptions of the gasifier design and operation are given in Gaston et al. [41]. Batch mode experiments were conducted at 800 °C using plain olivine and 650 °C and 800 °C with modified olivine. Each replicate experiment used 2.0 g of 0.7 mm diameter white oak as feedstock. Additional batch mode experiments were conducted at 600 and 700 °C using plain olivine; each replicate in these experiments used 8.0 g of 6 mm white oak as feedstocks. The amount of gases produced is normalized to the amount of biomass feedstock used. Earlier research on feedstock size dependence has shown that though the quantity of light gases and the quantity of tar produced can depend on feedstock particle size, the type of tars present is not dependent on feedstock size [42]. The amount of gases produced is presented as a function of biomass particle size in the results section.

In batch mode, a pulse of transient gas was produced when each batch of feedstock is gasified. Reaction gases measured were H_2, measured with a thermal conductivity detector (TCD), and CO, CO_2, and CH_4, each measured with a non-dispersive infrared detector (NDIR). The measured transient gas compositions were further integrated as a function of time to determine the total amount of gases evolved.

The gas stream exiting the gasifier was also flowed through a line heated at 500 °C to prevent tar condensation [40] and to allow real-time sampling of tars (<450 amu) by MBMS. With the MBMS system, the gases are sampled through a 250 μm orifice into a vacuum chamber maintained at 100 mTorr. The resulting adiabatic expansion effectively quenches reactions and cools the products, before the expansion is skimmed into a molecular beam in a second chamber (10^{-5} Torr) then ionized for mass spectrometry analysis in a third chamber (10^{-6} Torr). The MBMS spectra were normalized using the intensities of the argon tracer gas ($m/z = 40$), which was introduced at a constant flow of 60 sccm.

After several replicates of the experiments, air was flowed into the reactor to burn the char and any coke that was on the catalysts. The burnout was monitored by measuring CO_2 and CO gases with NDIR. The burnout process combusted char that might have accumulated on the catalyst surface and could have resulted in oxidation of the catalyst, though no effort was made to reduce the nickel after the burn-off.

2.3. X-ray diffraction

X-ray diffraction was conducted to obtain structural information about the freshly synthesized and post-reaction olivine samples. Spectra were acquired using a Rigaku spectrometer with a Cu Kα X-ray source and scanning a range of 3–120° 2θ with a step size of 0.02°. Powder diffraction files (PDFs) from the International Centre for Diffraction Data (ICDD) were used for diffraction assignments.

2.4. Scanning electron microscopy and energy dispersive X-ray spectroscopy

Scanning electron microscopy (SEM) was conducted using a FEI quanta 400 FEG instrument. The catalysts were mounted on 12 mm aluminum SEM pin-type stubs using double-sided carbon tape and coated with roughly 5 nm of iridium using a Cressington model 208HR sputter coater to ensure the samples where conductive. The materials were then imaged in high vacuum mode at electron energy of 20 keV with a working distance of 10 mm.

Samples appropriate for chemical localization studies were not coated and imaged in low vacuum mode utilizing a FEI quanta 400 FEG instrument coupled with an energy dispersive X-ray spectroscopy (EDS) system at 20 keV. Elemental spectra maps of the major elements Mg, Fe, Si, Ni, Ce, and O were also collected, tracking the same elements in order to understand the elemental localization within the catalysts.

2.5. Temperature programmed reduction

Temperature programmed reduction (TPR) was performed using an Altamira Instruments AMI-390. For the TPR experiments 100 mg of catalyst was packed into a quartz U-tube with quartz wool plugs at each end of the catalyst bed. During catalyst reduction 10% hydrogen in argon was run at a flow rate of 35 cc/min. The temperature was programmed to start at 50 °C and ramp to 900 °C at a rate of 10 °C/min then held for 30 min. The influent and effluent gas was analyzed using a thermal conductivity detector (TCD) that was set at 75 mA with a gain of 10. Data analysis was performed using Altamira's analysis package and Microsoft Excel.

3. Results

3.1. Gas yield and mass spectrometry measurements

Fig. 1 shows the carbon-based yield in the form of light gases (sum of CO, CO_2, and CH_4) and hydrogen-based yield in the form of H_2 produced at different gasification temperatures using plain and modified olivine. Fig. 1(a) shows the carbon-based yield. The yield is calculated in mole carbon in light gas per mole carbon in the oak feedstock. For plain olivine, increasing the temperature of gasification increases the carbon-based yield. Two different data points for the 800 °C data are presented, one obtained with oak spheres at a diameter of 6 mm, the other with oak spheres at a diameter of 0.7 mm. The carbon-based yield with the smaller diameter feedstock is higher, similar to the conclusions obtained in a detailed study of the impact of biomass feedstock particle size on syngas yield and tar production [41].

Fig. 1(a) also shows the carbon-based yield of light gases when modified olivine was used in the gasification experiments is higher than those obtained when plain olivine was used. This is clear at 800 °C, where for the modified olivine more than 90% of the carbon in the biomass is converted to light gases, while the carbon conversion with plain olivine is in the 70% range. At 650 °C, the carbon yield in the form of light gases is 73%, higher than that obtained with plain olivine at 600, 700, and 800 °C. Even if accounting for slightly higher carbon yield with plain olivine at smaller oak feedstock particle size at 600 and 700 °C, the yield with modified olivine in the lower temperature regions of 600–700 °C is higher than that with plain olivine.

The hydrogen in the product gas is predominantly in the form of H_2, CH_4, other hydrocarbons and tars. Since H_2 is the most important component for downstream synthesis of fuels or chemicals, we focus our analysis on H_2 yield. Fig. 1(b) shows hydrogen-based yield in the form of H_2 from the original hydrogen content in the

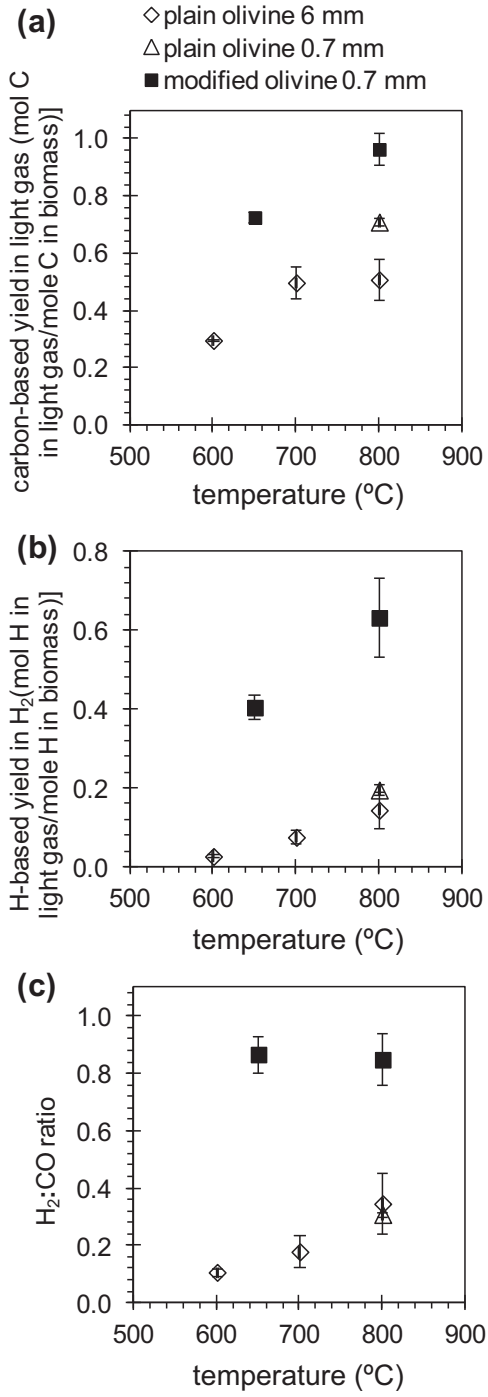

Fig. 1. Yields and H_2:CO ratio in the product gas as a function of gasification conditions. (a) Carbon-based yield in the form of light gas (CO, CO_2, and CH_4); (b) hydrogen-based yield in the form of H_2; (c) H_2:CO ratio in the product gas. For all three figures, solid squares show yield obtained when modified olivine is used as the fluidizing material, and empty diamonds and triangle show yield obtained when plain olivine is used as the fluidized bed material. The size information (e.g., 6 mm) in the legend that follows the fluidized bed material description (e.g., modified olivine) refers to the biomass feedstock diameter.

biomass. The original hydrogen content of the biomass is calculated as the sum of the hydrogen in the dry biomass and the hydrogen of the water in the biomass. In other words, in this calculation, the hydrogen content of the water in the biomass is assumed to be available for conversion into H_2. If the hydrogen-based yield is analyzed in terms of the hydrogen content of the biomass derived from

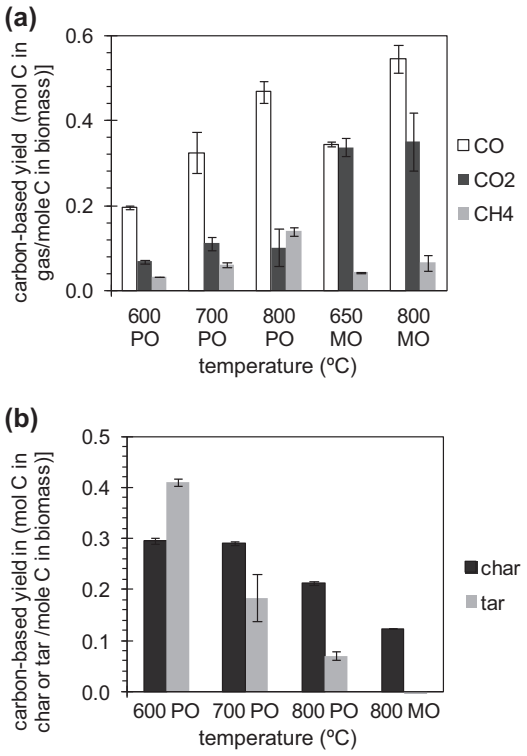

Fig. 2. Fraction of carbon in the original biomass being converted to (a) CO, CO_2, CH_4, and (b) char and tar. The conditions are labeled by gasification temperature followed by the type of fluidized bed material in the gasifier, with PO referring to plain olivine, and MO referring to modified olivine.

lignocellulosic components, the yield is higher by approximately 0.4–9%.

For plain olivine, increasing the temperature of gasification increases the hydrogen-based yield from 3 to 20% (Fig. 1(b)). The hydrogen produced with modified olivine is 40–63% of the original available hydrogen, significantly higher than when plain olivine is used in the gasifier (Fig. 1(b)). If the hydrogen-based yield was expressed as the number of moles of hydrogen in the form of light gases (H_2 and CH_4), then the yield with plain olivine ranges from 12 to 58% between 600 and 800 °C. With modified olivine, the yield ranges from 52 to 81% between 650 and 800 °C. Compared to the case where the hydrogen-based yield is expressed as the number of moles of hydrogen produced, the smaller improvement when modified olivine is used in this calculation is because of the substantial amount of CH_4 produced when plain olivine is used in the gasifier.

The H_2:CO ratios for the different gasification conditions are shown in Fig. 1(c). With modified olivine, the H_2:CO ratio is between 0.8 and 0.9 at both 650 °C and 800 °C, a significant increase compared to the case of plain olivine.

Fig. 2 shows speciation of the light gases produced as a function of temperature and fluidized bed material (plain olivine vs. modified olivine). Fig. 2(a) shows the fraction of the carbon in the biomass that is being converted to CO, CO_2, and CH_4. Production of CO and CH_4 increased with temperature when plain olivine was used as a fluidized bed material. This result is in agreement with the higher carbon conversion to light gas as temperature increases.

Comparing gasification at 800 °C with modified and plain olivine, the fraction of carbon being converted to CO and CO_2 both increased, by 17% and 240%, respectively. With plain olivine, the fraction of carbon being converted to CH_4 was 14%; with modified olivine, the fraction of carbon being converted to CH_4 was 7%. The decrease in the fraction of carbon being converted to CH_4 when

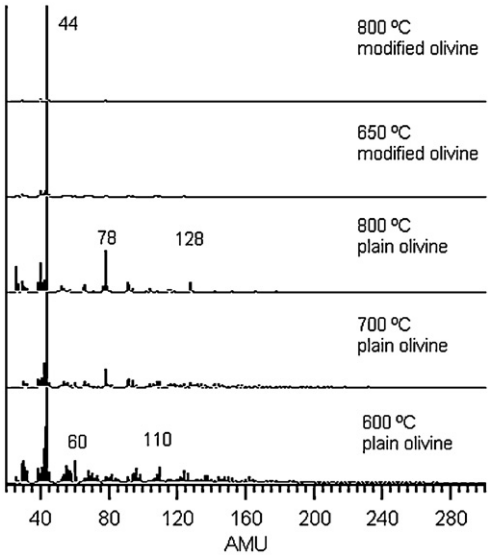

Fig. 3. Normalized, background subtracted MBMS spectra of the gas produced from gasification of oak feedstock at different gasification conditions.

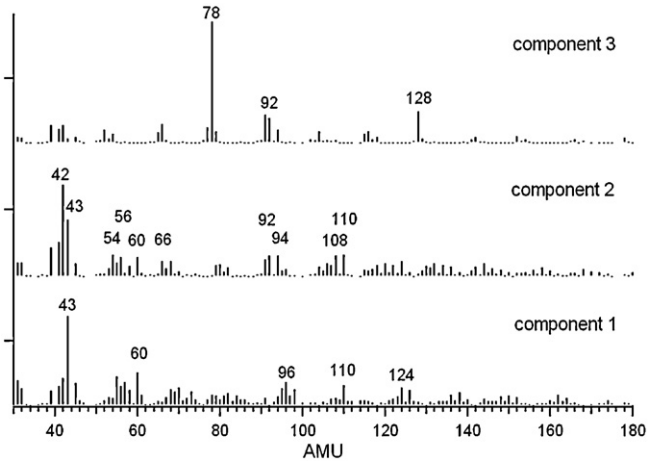

Fig. 4. Component spectra plot: this plot displays the estimated spectra of three pure constituents across all the variables included in the analysis.

modified olivine was used, coupled with the increase in the fraction of carbon being converted to CO and CO_2, resulted in a 70% reduction in the percentage of CH_4 in the product gas (CH_4 comprised 16% of the product gas composition when plain olivine was used, while CH_4 comprised 4.7% of the product gas composition when modified olivine was used). This result is significant as the modified olivine "tunes" the produced syngas composition for subsequent use downstream processes.

Fig. 2(b) shows the fraction of the biomass carbon being converted to char and tar. As described in the Methods section, the amount of char is determined by measurements of the CO_2 and CO evolved when conducting the burn off step after gasification. The fraction of biomass converted to tar is determined by the difference between the original available carbon and the sum of the light gas and char produced.

With plain olivine, the fraction of carbon that results in char production is approximately 30% at 600 and 700 °C, reducing to approximately 20% at 800 °C. The tar content likewise decreases from 40 to 7% of the original carbon content as temperature increases from 600 to 800 °C. Using MBMS measurements, it is shown that most of the "tar" at 600 °C is actually oxygenates that are released when biomass is pyrolyzed. That result will be described in more detail in Figs. 3–5.

With the use of modified olivine, the char produced at 800 °C is 12% of the original carbon, a 40% reduction compared to gasification at 800 °C using plain olivine. Within experimental uncertainty tar content was calculated as not present in significant amounts for gasification at 800 °C using modified olivine. An analysis of the MBMS data presented in later section (Fig. 5) shows a 70–80% reduction in tar content at 800 °C with modified olivine compared to plain olivine. The tar content for plain olivine at 800 C is 7% of the original carbon (Fig. 2), therefore the MBMS analysis would suggest a tar content of 1% with modified olivine at 800 °C, an estimate consistent with that calculated from the difference between original available carbon and the sum of the light gas and char produced. The char data for modified olivine at 650 °C were not collected.

Fig. 3 shows normalized raw MBMS spectra of the gases exiting the gasifier when gasification conditions are varied. For simplicity, only data in the amu range of 20–300 are shown. The normalization of the data was done so that all masses are expressed as a fraction of the total number of counts. For all the spectra, the dominant peak is AMU 44, which corresponds with mass unit of CO_2, acetaldehyde, N_2O, or propane. Since CO_2 is also measured with NDIR and is shown to have very high concentrations (percentage level), the majority of the AMU 44 peak in the MBMS spectra is likely from the contribution of CO_2.

The bottom three spectra in Fig. 3 are produced from gasification with plain olivine. Each of the spectra of gases produced from plain olivine at 600, 700, and 800 °C are different,

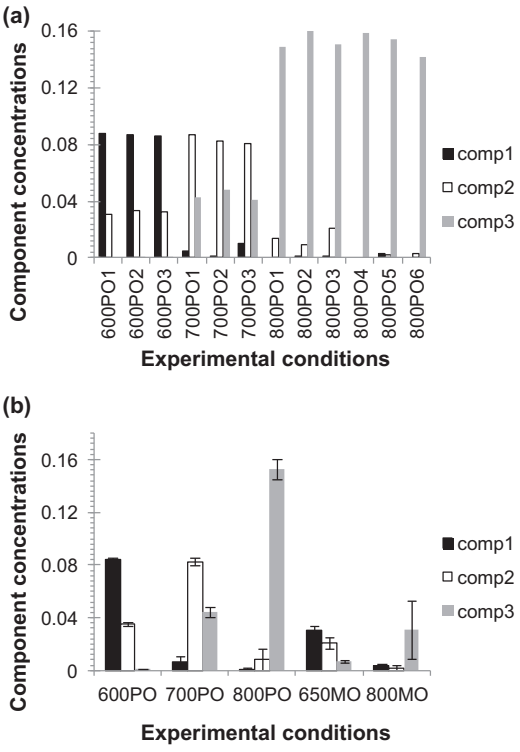

Fig. 5. Results of MCR analysis of the MBMS data of oak gasification with modified and unmodified olivine. This plot displays the estimated concentrations of two or more constituents across all the samples included in the analysis. Each plotted curve is the estimated concentration profile of one given constituent. (a) Component concentration plot of gasification with plain olivine at 600, 700 and 800 °C, highlighting the changes in the dominant pure component as gasification temperature changes. (b) Average component concentration of gasification with modified and plain olivine at different temperatures, error bars represent standard deviation of the component concentrations. The conditions are labeled by gasification temperature followed by the type of fluidized bed material in the gasifier, with PO referring to plain olivine, and MO referring to modified olivine.

Table 2
Prominent ion peaks in components 1–3. This list is meant for highlighting some of the major peaks rather than being exhaustive. The assignment of possible compounds are largely based on the work of Evans and Milne [39]; certain assignments with references to additional studies are also shown.

Component	Ion, m/z	Formulas	Possible compounds
1	43, 57, 73, 85		Fragment ions from pyrolysis of carbohydrates [39,44]
	58	C_3H_6O	2-Propanone (acetone)
	60	$C_2H_4O_2$	Acetic acid, hydroxyacetaldehyde, methyl formate
	68	C_4H_4O	Furan
	82	C_5H_6O	2-Methylfuran, cyclopentenone
	94	C_6H_6O	Phenol
	96	$C_5H_4O_2$	Furfural
		C_6H_8O	2-Methyl-2-cyclopentene-1-one
	98	$C_5H_6O_2$	Furfuryl alcohol
			Fragment of levoglucosan [45]
	110	$C_6H_6O_2$	5-Methylfurfural
			Dihydroxybenzenes (catechol, hydroquinone, resorcinol)
	124	$C_7H_8O_2$	2-Methoxyphenol
		$C_8H_{12}O$	Trimethylcyclopentenone
	126	$C_6H_6O_3$	5-(Hydroxymethyl)-2-furfural
			2-Methyl-3-hydroxy-4-pyrone
	138	$C_8H_{10}O_2$	4-Methylguaiacol
2	42	C_3H_6	Propene
	54	C_4H_6	Butadienes, butyne
	56	C_4H_8	Butenes
	66	C_5H_6	Cyclopentadiene
	92	C_7H_8	Toluene
	94	C_6H_6O	Phenol
	108	C_7H_8O	Cresol
	110	$C_6H_6O_2$	Dihydroxybenzene
3	78	C_6H_6	Benzene
	92	C_7H_8	Toluene
	128	$C_{10}H_8$	Naphthalene

with the gases produced at 600 °C containing a series of peaks clustering around 43, 60, and 110 AMU. At 800 °C, the peaks at AMU 78 and 128 become more dominant. Based on literature, all of these peaks are associated with tar molecules and the detailed assignments are discussed in Section 3.2 and shown in Table 2.

The top two MBMS spectra in Fig. 3 are produced from gasification with modified olivine. With the use of a modified olivine, the intensities of peaks associated with tar molecules are significantly reduced at both 650 and 800 °C, though the reduction of the tar-molecule peaks are also accentuated by the normalization method because the CO_2 peak (AMU 44) increased substantially when modified olivine was used.

3.2. Multivariate analysis of MBMS data

Multivariate curve resolution (MCR) was used to analyze overall trends in the MBMS data. The Unscrambler X software package (version 10.1, Camo Software) was used for this analysis. The data set used included all the replicates for the plain olivine and modified olivine experiments (29 total). The 600 and 700 °C plain olivine spectra are from 6 mm size feedstock, while the rest of the data are from 0.7 mm size feedstock. An earlier study on the impact of biomass particle size on gasification shows that the particle size affects the amount of tars, but not the type of tar molecules. Therefore the inclusion of data from these two size ranges is justified.

Mass spectra from AMU 30 to 300 were used in the MCR analysis in which normalization of all masses was conducted with the exclusion of the CO_2 peak. This accentuates the other peaks associated with the tar molecules for classification purposes. Several AMUs were excluded because the signals were below the noise levels or because the signal were very large and dominate, e.g., AMU 28, which came from the contribution of N_2 and CO, as well as AMU 44, which came primarily from the contribution of CO_2.

The MCR analysis indicates that three pure constituents best describe the variance in the data set and the results are similar to those of biomass pyrolysis studied by Evans and Milne [39] and gasification with plain olivine conducted by Gaston et al. [41]. Fig. 4 shows the estimated spectra of the three pure constituents across all the variables included in the analysis. The probable assignments of the m/z values dominant in these components are shown in Table 2, with the assignments principally based on previous work [39,43–45], which in turn were made based on cross correlations with other analytical methods, isotopic labeling, and pyrolysis of individual fractions of biomass (e.g., pyrolysis of pure cellulose or glucose). The first pure constituent or first component consists of peaks from carbohydrates and lignin deconstruction products. The second pure constituent or second component consists of peaks that are usually interpreted to be further cracking products of the first pure constituent. The third pure constituent consists of peaks that are associated with polycyclic aromatic hydrocarbons.

The concentrations of these three components as a function of gasification conditions, another result of the MCR analysis, are presented in Fig. 5. Fig. 5(a) shows the component concentrations as a function of temperature, when plain olivine was used in the gasifier. Every replicate in the plain olivine experiments is shown with the caption indicating the temperature, the type of olivine used, and the replicate number. For example, 600PO1 indicates gasification at 600 °C, with plain olivine, and it is the 1st replicate of the experiments. The plot shows that within each temperature, the component concentrations are reproducible from one replicate to the other. The first component is dominant at 600 °C; the second component is dominant at 700 °C, while the third component is dominant at 800 °C. This finding is in agreement with earlier research on the impact of temperature on the gas phase composition derived from pyrolysis and gasification [39,45].

Fig. 5(b) shows the component concentrations when either modified olivine or plain olivine was used at several different temperatures. In order to simplify the plot, after the MCR analysis of all replicates was conducted, the average component concentrations at each condition is calculated and then plotted. Overall, the relative abundance of the three components at 650 °C with modified olivine are more similar to that of gasification with plain olivine at 600 °C,

i.e., there is a higher concentration of component 1 than component 2, which in turn has a higher concentration than component 3 (Fig. 5(b)).

Earlier research by Jarvis et al. [45] and Gaston et al. [41] show that the characteristic of the gas at a mid-point temperature such as 650 °C is approximately a composite of those at 600 and 700 °C. Therefore, the concentrations at 650 °C with plain olivine can be approximated by the mid-point of those with plain olivine at 600 and 700 °C. Comparing the component concentrations of gasification with modified olivine at 650 °C with an average of those of plain olivine at 600 and 700 °C, there is inconclusive evidence whether component 1 decreased when modified olivine is used at 650 °C. Since most of the "tar" molecules at that temperature are oxygenates (Fig. 4), the result suggests that the Ni–Ce modified olivine is not as effective deoxygenating these oxygenates, i.e., convert the oxygenates to hydrocarbons, which are more typically present in component 2.

There is, however, strong evidence that at 650 °C, components 2 and 3 decreased. This result, coupled with earlier finding that the fraction of carbon being converted to light gases at 650 °C with modified olivine is 1.5 times that of the carbon conversion at 700 °C with plain olivine (and 2.4 times that of the carbon conversion at 600 °C with plain olivine), suggest that the increased light gas conversion is derived from the reforming of tars in components 2 and 3 and breaking up of char or blocking the formation of tars and char at that temperature.

Fig. 5 shows that at 800 °C, compared to gasification with plain olivine, components 2 and 3 decreased by 80% when modified olivine is used. The low concentrations of molecules in pure constituents 1–3 are in agreement with the low tar content determined by mass balance.

An alternate way of quantifying tar reduction is by using well-known tar molecules for indexing. For example, benzene, naphthalene, and phenanthrene are typically considered the most prominent tertiary tar or members of component 3. By summing the mass spectrometry intensities of those three molecules at 800 °C, we found that these three molecules were reduced by more than 70% when comparing the case of using modified olivine to plain olivine.

3.3. XRD results

The XRD results of the pre- and post-reaction catalyst are shown in Fig. 6. Analysis of the freshly synthesized Ni-olivine catalysts indicates that the dominant X-ray diffraction spectrum is best fitted with synthetic olivine ($MgFe(SiO_4)$), at 2θ of 23.86°, 32.23°, 35.63°, 36.47°, 38.29°, 39.66°, 52.52°, 56.88°, 82.74°, and 92.70°. In addition to olivine, there is an additional silicate phase, enstatite ($Mg_{1.83}Fe_{0.17}Si_2O_6$). The XRD peaks of enstatite are at 28.50°, 31.14°, 35.72°, 36.47°, 39.66°, 43.28°, 47.45°, 48.48°, 58.65°, 62.75°, and 67.04°. Some of the peak positions of enstatite overlap those from olivine. In the fresh modified olivine, there are two peaks at 38.3° and 38.8° that can be attributed to olivine or magnesium nickel silicate, $Mg_{0.969}Ni_{1.02}(SiO_4)$. The 2θ values for those two compounds are very close at about 38.3° and 38.8°.

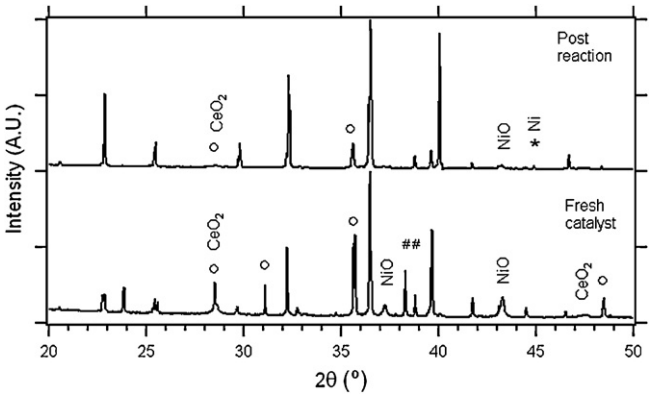

Fig. 6. XRD results of the catalyst pre- and post-reaction. The peaks that are unmarked are from olivine reflections. The peaks marked with the ○ symbols are enstatite. The two peaks marked # can be from olivine or magnesium nickel silicate. The other peaks are specifically marked for the mineral phases they represent.

After gasification with the modified material, the line positions of olivine stayed largely intact. The XRD lines that are uniquely enstatite, however, were weaker.

A nickel oxide phase was detected on the fresh catalyst, with main peaks at 37.26°, 43.28°, and 62.75°. It is also possible that some Mg from the host material has substituted for Ni sites during the calcination process, thus the structure detected could also be (Ni,Mg)O, which has been discussed in literature [28].

After the reactions, the intensity of the NiO or (Ni,Mg)O peaks decreased. A small nickel or Fe peak appears at 44.9°, 85.2°, and 86.5°. These peaks were not detected prior to catalytic gasification, and they can potentially be attributed to Ni, Fe, or a Ni–Fe alloy, since these three materials are isostructural.

A cerium oxide phase, CeO_2, was detected on fresh catalyst, with major peaks at 28.50° and 47.45°. The 28.50° peak overlaps with an enstatite peak. After the reaction, the intensity of the peak at 28.50° decreased significantly. Because the other main enstatite peak at 35.72° also decreased significantly after the reaction, it is safe to conclude that the enstatite phase decreased after the reaction. However, it is harder to determine whether CeO_2 decreased or formed other phases after the reaction because the other main CeO_2 peaks, e.g., the one at 47.5°, are quite weak to begin with, most likely due to the low percentage of cerium in the catalyst.

Thus, the overall conclusions are that olivine support was largely unchanged after gasification. Enstatite decreased after the reaction. Some of the NiO was converted to Ni. There is also the potential of some elemental Fe formation after catalytic gasification reaction. If there were any changes to the CeO_2 phase, they could not be determined conclusively. Since CeO_2 is a refractory material, it is likely that it remained as CeO_2 or was converted to CeO_x, with $x < 2$. The implications of these phase changes will be discussed in more detail in later sections.

3.4. Catalyst morphology, metal distribution, and BET surface areas

The surface area of the fresh nickel cerium modified olivine catalyst, according to Kr-BET measurement, was only 1.5 m^2/g. After gasification, the Kr-BET surface area decreased to 0.7 m^2/g.

SEM–EDS shows that the olivine particles tended to be nonporous and have angular ridges and edges (Fig. 7). The SEM–EDS results of nickel cerium modified olivine show that the nickel particles are quite large. In other images, the nickel seemed to have a preference for some of the edge areas of the olivine particles (Fig. 8). There did not seem to be any association between nickel and ceria.

3.5. TPR data

The temperature programmed reduction data are shown in Fig. 9. The fresh catalyst has its main reduction peak at 378 ± 5 °C, and a shoulder at approximately 280 °C. For the post-reaction catalysts, the reduction profile has changed, with the reduction peak now at approximately 433 ± 10 °C, and the "shoulder" becoming significantly less prominent. This suggests the easily reducible fraction of the catalyst was already reduced during the gasification

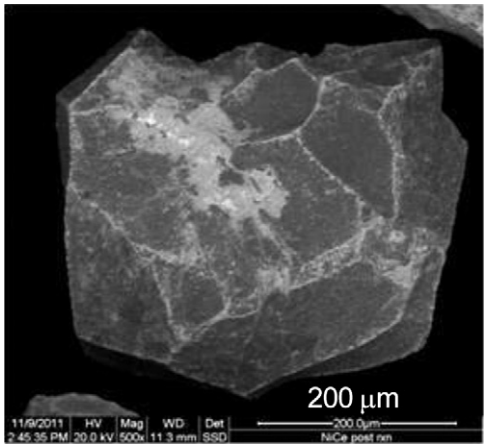

Fig. 7. An SEM micrograph of a typical nickel cerium modified olivine particle.

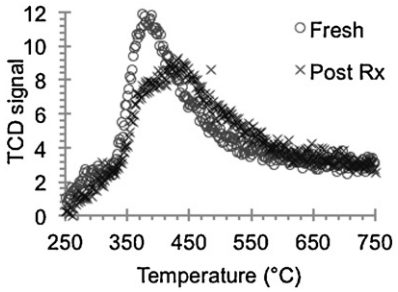

Fig. 9. Temperature programmed reduction of the fresh and post-reaction catalysts.

experiments and the remaining fraction is not reduced until higher temperatures.

4. Discussion

4.1. Heterogeneity of the catalyst support

In XRD analysis of our as-received olivine, though the XRD patterns occur in the same 2θ, there can be large variation in the peak intensities of those XRD peaks from one batch to other. This is in agreement with the olivine being a natural mineral, which can readily be altered in H_2O-containing environment into serpentine such as antigorite ($Mg_6Si_4O_{10}(OH)_8$), magnesite ($MgCO_3$), and iron oxides [46]. The incorporation of some of these impurities into our olivine sample is probably the main reason for some of the batch-to-batch variation in peak intensities. However, the primary contributions to the XRD patterns we observed are still from olivine and enstatite.

4.2. In situ reduction of catalyst during catalytic gasification

The XRD analysis also showed that after the catalytic gasification experiments, the peaks corresponding to nickel oxide (or mixed magnesium nickel oxide) had decreased in intensity and new peaks at the 2θ positions of Ni or Ni–Fe alloy have appeared. In the XRD results, the CeO_2 peaks decrease in intensities. However, there is not sufficient evidence to suggest the formation of Ce_2O_3. Nevertheless, there could be formation of CeO_x, where x is less than two.

Our results showing the formation of metallic Ni or metallic Fe–Ni in the reducing environment of biomass syngas is in agreement with what is known about olivine in nature. Olivine is a well-studied mineral and geologists have found that chemical zoning in olivine with Mg-rich cores and more Fe-rich rims sometimes occur in high temperature igneous rocks [46]. The Fe-rich rim means there is a slight abundance of Fe on the surface of olivine to react with other metallic species and potentially contribute to tar-reforming activity, even when the olivine is not modified. With the use of electron microprobe geologists have also observed substitution of nickel into natural olivine and formation of Fe–Ni metallic precipitates under reducing conditions [47].

Kuhn et al. found the presence of both (Ni,Mg)O and metallic Ni, Fe, or alloy after thermal impregnation of the catalyst [28]. In addition, the intensities of the (Ni,Mg)O and metallic Ni, Fe, or alloy XRD peaks are largely unchanged in a reducing environment [28]. In contrast, we do not see evidence of metallic species after the aqueous impregnation procedure and observed the appearance of metallic species only after the catalyst was used for catalytic gasification. These differences might be due to the different catalyst calcination conditions (calcination in Ar at 1400 C in Kuhn et al. vs. calcination in air at 800 °C in our case) or perhaps the higher iron content of the olivine used in the Kuhn et al. preparation (10% vs. 4% in our case).

The finding of in situ reduction of NiO to metallic Ni or Ni–Fe alloy is important because the metallic form of catalyst such as Rh, Pt, Pd, Ru, and Ni are the active form to catalyze C—H and C—C bond scissions of hydrocarbons that are challenging to activate (such as methane or ethylene). Previous research by Kuhn et al. showed that metallic Ni is the active species in the reforming of hydrocarbon such as ethylene but the contribution of Ni (compared to plain olivine) to methanol reforming is minimal [28].

In situ reduction of NiO is also important because the oxygen released by the catalyst has an impact on the light gas yield and coke formation. This aspect will be discussed in more detail in later

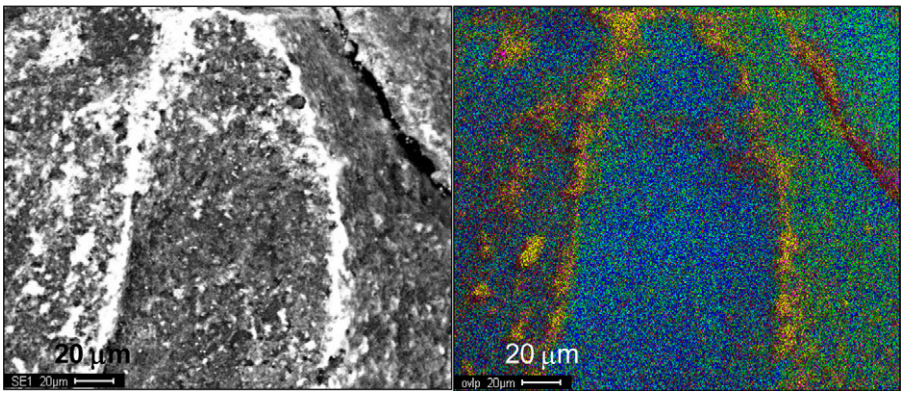

Fig. 8. SEM and EDS images of Ni (yellow), Ce (magenta), Mg (blue), Si (teal/green) on olivine.

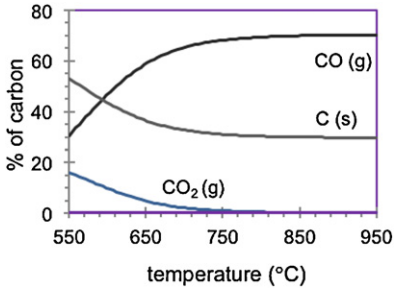

Fig. 10. Thermodynamic calculation results of carbon speciation in the biomass gasifier using biomass elemental composition as input with no additional oxygen source. Though not shown, the calculation also predicts the amount of other gas and solid species, with H_2 and H_2O being the other two major species.

sections. Lastly, technoeconomic modeling has suggested that an indirectly heated circulating fluidized bed gasifier can be an economical process option [48,49]. In this operation mode, the material in the fluidized bed will need to be cycled between gasification and combustion (of coke) stages continually. A catalyst in the form of fluidizing bed material that does not require prior reduction when it is being cycled back from the combustor stage to the gasifier will require no external hydrogen input and is economically beneficial to the biomass gasification process.

4.3. Coke and char formation and oxygen source

Because of the low hydrogen to carbon ratio in biomass, the heating of biomass in the absence of nitrogen tends to produce coke. In order to reduce coke formation, an external hydrogen or oxygen source is required. This external oxygen source in gasification is often supplied in the form of water or oxygen, and the impact of steam to biomass ratio or steam/air to biomass ratio in gas yield has been extensively studied [50–52].

Our experimental result shows approximately 20% char/coke production at 800 °C with plain olivine, and 12% char/coke at 800 °C with modified olivine. A simple thermodynamic calculation was conducted to determine the theoretical predicted char/coke content under our experimental conditions. An equilibrium calculation does not include mechanisms of tar formation or biomass conversion, but rather, serves to identify possible driving forces in this complex system and to suggest possible directions to improve the process. For this calculation, the HSC Chemistry software package (version 6.1, Outotec Research) was used to predict the equilibrium product distribution based on the elemental composition of the biomass. Because the thermodynamic data for biochar are not readily available, we use graphitic coke as an approximation in the calculations.

Fig. 10 shows predicted carbon distribution using the biomass elemental composition as the input for the HSC thermodynamics calculations. The model predicted close to 30% coke at 800 °C. In other words, the experimentally determined amount of coke/char produced is less than that predicted by a simple thermodynamic model. This discrepancy could be due to uncertainty in the Gibbs free energy of formation of various components in the products or it could be due to additional hydrogen or oxygen sources that were not taken into account in the preliminary model.

In addition to the discrepancy between model and experimental results of the extent of char/coke formation, the experimental data also show significantly higher CO_2:CO ratio than model prediction. The amount of CO_2 in the modified olivine experiments is also high relative to those found in experiments performed with plain olivine. Carbon monoxide or carbon can be a reductant for metal oxide, producing CO_2 in the process. To test this

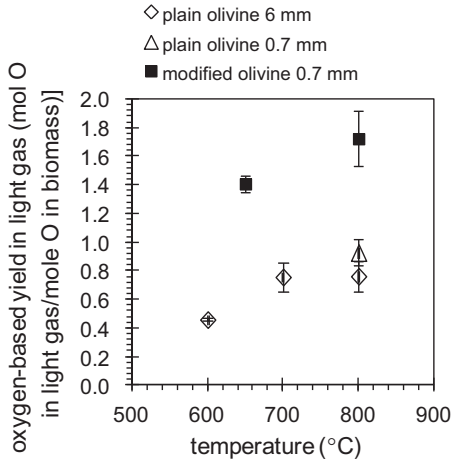

Fig. 11. Oxygen ratio expressed in terms of total number of moles of oxygen in CO and CO_2 in the light gases produced per mole of oxygen in biomass. In the calculation of the number of moles of oxygen in the biomass, oxygen in the water content of the biomass is included.

hypothesis, we conducted an "oxygen balance" and further thermodynamic modeling

Because of the challenge in measuring the H_2O content in the syngas produced, we were not able to do a complete oxygen mass balance for the pyrolysis/gasification reactions. We are, however, able to calculate the ratio of oxygen in the light gases (sum of CO and CO_2) to the original available oxygen in the biomass; this ratio will be termed oxygen ratio. In the calculation, we assume the oxygen in the water content of the biomass is available for reaction, in the same way we did the calculations for hydrogen conversion efficiency.

Fig. 11 shows the results of this calculation. In plain olivine, the oxygen ratio increased with temperature, with the highest value of the "oxygen conversion efficiency" being 1.0. In modified olivine, the oxygen ratio is 1.4 at 650 °C, and 1.7 at 800 °C. These values suggest that even when just counting the oxygen in CO and CO_2 (i.e., not counting the oxygen in H_2O in the product gas), the amount of oxygen in the gases produced when modified olivine was used is more than that originating from the biomass itself. Since the gasification was conducted with no additional oxygen source in the form of O_2 or H_2O, the additional oxygen is derived from the reduction of the catalyst, according to the two reactions:

$$MO(s) + H_2(g) = M(s) + H_2O(g)$$

$$MO(s) + CO(g) = M(s) + CO_2(g),$$

where M stands for a metal. The oxygen ratio with plain olivine is 1.0, so it does not provide evidence for or against the potential of having an oxygen donor. Nevertheless, Swierczynski et al. showed that the fraction of the iron in olivine can be present in the form of reducible iron oxide [27]. More recently Virginie et al. found that Fe-enriched olivine can act as an oxygen carrier that transfers oxygen from a combustor to a gasifier in a dual fluidized bed system [18]. In our current study, in addition to olivine, the as-prepared catalyst contains both NiO and CeO_2. Nickel oxide has been proposed as an oxygen carrier for chemical looping combustion [53], while CeO_2 is known to contribute to oxygen transport and storage [54]. All of these minerals (nickel oxide, cerium oxide, and iron oxide) have the potential to contribute oxygen to the gasification reactions. Our preliminary modeling suggests nickel oxide is the most readily reducible among the three.

Additional thermodynamic modeling was conducted assuming there was equal number of moles of NiO as the carbon available.

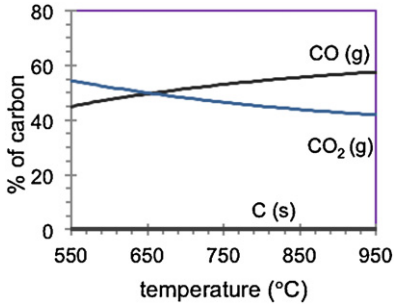

Fig. 12. Thermodynamic prediction of the carbon speciation in the gasifier assuming equal number of moles of NiO as carbon available.

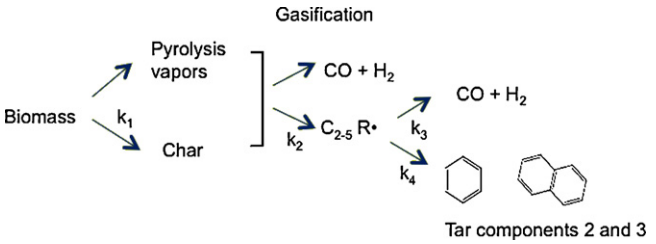

Fig. 13. Pathways for tar formation based on literature reports. Two potential pathways can explain the reduction in tar observed when modified olivine is being used. One is that the modified olivine block the pathway from C_{2-5} radicals to tars, the other is that the modified olivine is active at catalytically reforming tars being formed within the gasifier.

Fig. 12 shows predicted equilibrium carbon distribution assuming sources of oxygen from NiO, with the catalyst to biomass ratio equal to one. The model shows that the predicted char and coke content with that amount of NiO is practically zero (Fig. 12). The same model shows that the equilibrium nickel containing phase from 550 to 950 °C is metallic nickel. At the catalyst to biomass ratio used for the calculation, the predicted CO to CO_2 ratio at 800 °C is 1.2, compared to the experimental 1.55, and the predicted CO to CO_2 ratio at 650 °C is 1.0, compared to the experimental value of 1.0. In other words, the CO to CO_2 ratio observed experimentally can be mostly explained as a result of reduction of the metal oxide catalyst. The reduced coke/char formation when modified olivine was used is also consistent with thermodynamic prediction of an additional oxygen source.

4.4. Comparison to literature results and future system optimization

Our results show that at 650 °C, the carbon yield based on the light gas data averages 70%. The results compare very well with those obtained with a nickel aluminate catalyst reported by Garcia et al., which reported light gas yield of 70% for dry gasification with Ni-aluminate at 700 °C [20,22]. At 800 °C, our carbon yield based on the light gas data averages 90%, indicating high conversion of the original biomass to the gas. With the modified catalyst, the light gas yield at 800 °C is almost 30% more than the yield at 650 °C.

The model results in Fig. 12 suggest that with the catalyst oxygen source, the carbon loss in char/coke is minimal even at the low temperature of 650 °C. Nakamura et al. reported carbon yield ranging from 70% to close to 80% for steam gasification of cedar wood at a low temperature of 600 °C using nickel platinum catalysts [55]. The catalysts used in the Nakamura study were reduced ex situ. At a higher temperature of 700 °C, Garcia et al. also reported that steam gasification with catalyst present results in carbon yield of 90–100%.

These experimental results show that with modified fluidized bed material as catalyst, gasification at lower temperature ranges, e.g., 700 °C, is possible. Conventionally, biomass gasification is conducted at high temperature range, e.g., 800 °C and higher. This is partly because the kinetics of reactions are faster at the higher temperature so more biomass is converted to product gas, and the tar content of the product gas is lower. With catalyst which helps to increase the kinetics of reactions it may be possible to reach the predicted equilibrium composition at lower temperature in the 650–700 °C range.

As shown in Fig. 1(c), the H_2:CO ratio with modified olivine is between 0.8 and 0.9 for both the 650 °C and 800 °C experiments. In comparison, outlet gas from a downstream/secondary tar and methane steam reformer has been reported to have a H_2:CO ratio of approximately 1.2 [48]. Since our current work did not use steam, which is well known as a process condition that increases H_2:CO ratio in the gasifier outlet, we should be able to increase the H_2:CO ratio in future tests with steam present. We should point out that H_2:CO ratio is not a sufficient criterion by itself, since a product gas stream that has high CO_2 content would be equivalent to a gas stream that has low CO content, and consequently high H_2:CO ratio. As discussed in Section 4.3, the CO_2:CO ratio in our gas stream is high because of the reduction of metal oxide catalyst by CO.

To minimize CO_2 and maximize CO, the gasification process and the catalyst will need further optimization. Using a simple thermodynamic model as the one used in Fig. 12, it is estimated that the use of a lower catalyst to biomass ratio and a steam to biomass ratio of 0.1 is sufficient to significantly reduce char production. In future studies, steam will be incorporated into the catalytic gasification experiments to determine whether we can reduce CH_4 and tar further while minimizing CO_2 formation in the gasifier itself. Process conditions such as the use of catalyst, addition of small amount of steam as a fluidizing agent, or longer gas residence time in the gasifier are all possible routes that can bring the product gas closer to thermodynamic prediction.

4.5. Proposed pathways for tar, methane, and char reduction

Fig. 2 shows that with the use of modified olivine, production of char, tar, and methane is reduced. Fig. 2(b) shows that with modified olivine at 800 °C, the fraction of carbon being converted to char/coke is reduced by 40% compared to plain olivine. There are at least two types of char/coke in the gasifier. The first type of char forms directly from a biomass particle—there is evidence that when a biomass particle is heated, it attains a metaplastic stage, which later evolves into a swelling, gas releasing, foam-like char [45]. Another type of char/coke forms when a carbon-containing molecule adsorbs on a particle surface, e.g., graphitic carbon can form when CH_4 adsorbs on certain metallic surfaces. The formation rate of char derived directly from biomass particles may not be affected by solid catalyst particles. However, the formation rate of char that forms on olivine surface can be affected significantly by olivine modification. For simplicity, only one rate constant for char formation, k_1, is indicated in Fig. 13.

In addition, when the catalyst is being reduced in situ, oxygen is released in the form of either H_2O or CO_2, which plays a role in the oxidative atmosphere of pyrolysis and gasification. With CO_2, the reverse Boudart reaction (CO_2 (g) + C (s) = 2CO (g)) can occur and contribute to decrease in char content and overall improvement in the degree of conversion of biomass. However, there are insufficient data to indicate the relative significance of the reverse Boudart reaction vs. changes in the kinetics of char formation when modified olivine is used.

In addition to char reduction, measured tar concentration also decreased when modified olivine was used. This may be because the catalyst has an impact on the tar formation rate in the gasifier, or it may be because the catalyst is reforming tars that are already

formed. In the biomass literature significant research has been conducted on the mechanisms of tar formation. It has been proposed that gasification of char and pyrolysis vapors produce C_{2-5} radicals (C_{2-5} $R^{\bullet}$), which are then converted to tars [56]. One potential pathway for the reduction in tars, particularly tertiary tars, is for the catalyst to reduce the tar formation rates, i.e., the catalyst could decrease k_2 and k_4 in Fig. 13. The catalyst could potentially have a null or positive impact on k_3, which could help explain the observation of increased hydrogen yield in the presence of modified olivine.

The other potential pathway for the catalyst to decrease tar would be for the catalyst to reform tars that have already formed in the gasifier. Based on the multivariate analysis, the catalyst reduces components 2 and 3 at 800 °C by close to 80% (Fig. 5). These two sets of tar molecules comprised primarily of toluene, phenanthrene and anthracene are rich in C—C and C—H bonds. In contrast, the impact of the catalyst on component 1, primarily oxygenated pyrolysis products is inconclusive. At the lower temperature of 650 °C, most of the "tar" molecules (component 1) or pyrolysis products still contain oxygen. Within statistical error, in the conditions used in this work, the catalyst is not active in rejecting the oxygen for hydrocarbon formation, though the catalyst is active in improving yields of CO and CO_2 at that temperature. In other words, the Ni–Ce enriched olivine is active in C—C bond scission and reforming reactions rather than deoxygenation reactions at the conditions used in our current research. This is in agreement with findings by Kuhn et al. that nickel enriched olivine has a larger effect on the catalytic reforming of C_2H_4 as compared to oxygenated molecules such as methanol [28]. However, reforming experiments conducted outside of a gasifier cannot narrow down on the mechanism of tar reduction in the gasifier itself, so both the pathway blocking mechanism and the tar reforming pathways are possibilities.

Fig. 2 shows that in our current study in dry gasification mode at 800 °C, with plain olivine CH_4 comprised 16% of the product gas, while with modified olivine CH_4 comprised 4.7% of the product gas. The use of modified Ni–Ce olivine as fluidized bed material resulted in a 70% reduction of CH_4 in the product gas relative to when plain olivine was used as fluidized bed material. In comparison, with plain olivine (Austria plain olivine) at a steam to biomass ratio of 0.6 (by weight), CH_4 comprised 10.8% of the product gas; with modified Fe-enriched olivine at the same steam content, CH_4 comprised 10.2% of the product gas [18]. The use of Fe-olivine resulted in a 6% reduction of CH_4 content in the product gas. The Fe-enriched olivine was more active in tar reduction; it reduced tar content by 30% [18]. The larger reduction of tar and methane with Ni–Ce modified olivine is probably a result of the effectiveness of nickel for activating hydrocarbons that are more challenging to reform. It is possible that certain chemical synthesis from biomass may not require significant CH_4 reduction. In those cases, catalyst that has low CH_4 reforming activity may be sufficient. However, if CH_4 reduction is required for the process and if it was deemed economically advantageous to eliminate a downstream CH_4 reformer, then a catalyst in the gasifier that is highly active in methane reforming, i.e., catalysts containing Ni, Ru, Rh, or Pt [57] will most likely be necessary.

4.6. Technoeconomic implications

In a technoeconomic analysis of the feasibility of gasification of biomass followed by mixed alcohol synthesis, it was estimated that a reformer downstream of the gasifier needs to be able to reform 99% of the C_{10+} tars and 80% of the CH_4 [48]. Our current catalyst and configuration still do not completely meet the targets, but they are not significantly off (70–80% tar reduction vs. the target of 99% tar reduction, and 70% CH_4 reduction vs. the target of 80% CH_4 reduction). Since the dry gasification mode we used in our research is expected to produce syngas with higher tar and char content, it is highly likely that future research using steam in the gasifier can produce syngas with even lower tar content. If future research on catalyst and process improvement results in 99% reduction in the tar, it can potentially eliminate the need for a secondary tar reformer. Since tar reforming comprises approximately 9% of the total installed equipment cost [58], a reduction in the number of unit operations will decrease capital cost and improve the process economics.

It should be pointed out that the 80% CH_4 reduction target was established in the context of mixed alcohol synthesis from syngas [48]. For biofules other than alcohols, the CH_4 reduction requirement may be different. In addition to tar and hydrocarbon reduction, catalytic gasification has the further advantage of char reduction. Raw biomass is a significant contributor to the cost of biofuel, e.g., in the case of ethanol production from lignocellulosic material, biomass is estimated to contribute to 35% of the minimum ethanol selling price [48]. A reduction in char would result in improved yield and is equivalent to less biomass being needed for biofuel synthesis. The advantage of char reduction provided by catalytic gasification is a unique feature that cannot be provided by a downstream reformer, unless the char is reformed in a separate reactor. Char reduction in catalytic gasification is a factor that should be included in future technoeconomic analysis.

Earlier research has shown that larger biomass particle as feedstock produces more tars and reduces syngas yield [41]. Larger biomass particle is considered important for the economics of biofuel. One of the potential advantages of catalytic gasification is that it might reduce tar and improve gas yield for feedstock of large particle sizes.

5. Conclusions

At 800 °C, with catalyst in place, approximately 90% of the biomass was converted to light gas, with a 40% reduction in char, 70% reduction in methane, 80% reduction in secondary and tertiary tar content, three-fold increase in hydrogen yield, and 36% increase in the fraction of carbon being converted to light gases. The results were obtained using catalyst that was not reduced to the metallic form prior to the reaction, but rather, our analysis shows that the catalyst was reduced in situ rapidly by the product gas of biomass gasification.

The catalyst either reforms CH_4 or impedes CH_4 formation from its precursors. The high ratio of CO_2 to CO is not favorable for fuel synthesis, and future research will need to be conducted to reduce the CO_2 levels in favor of CO formation. The results show that catalytic gasification holds great promise to improve the efficiency of the biomass conversion process.

In this preliminary work, the synthesis method and the activity of the catalysts have not been optimized. Further optimization of the synthesis could potentially produce material with higher activity that can reduce tar further. This can occur through ways to load higher content of the active material to the support. Other challenges in the development of an active catalyst lie in improving the catalyst activity without prior reduction and enhancing the stability of catalyst to attrition, sintering, and deactivation by char and other inorganic molecules in the gasifier during extended use and multiple regeneration cycles.

Acknowledgements

Funding for this research was provided by the Office of the Biomass Program, U.S. Department of Energy, under contract number DE-AC36-99GO10337 with the National Renewable Energy

Laboratory. We gratefully acknowledge help on the use of the Unscrambler X Software from our colleagues Dr. Robert Evans, Ms. Whitney Jablonski, and Dr. Calvin Mukarakate; and ICP analysis conducted by Mr. Steve Deutch.

References

[1] T. Damartzis, A. Zabaniotou, Renewable and Sustainable Energy Reviews 15 (2011) 366–378.
[2] R.P. Anex, A. Aden, F.K. Kazi, J. Fortman, R.M. Swanson, M.M. Wright, J.A. Satrio, R.C. Brown, D.E. Daugaard, A. Platon, G. Kothandaraman, D.D. Hsu, A. Dutta, Fuel 89 (2010) S29–S35.
[3] G.R. Moradi, S. Nosrati, F. Yaripor, Catalysis Communications 8 (2007) 598–606.
[4] M. Mohammadi, G.D. Najafpour, F. Younesi, P. Lahijani, M.H. Uzir, A.R. Mohamed, Renewable and Sustainable Energy Reviews 15 (2011) 4255–4273.
[5] C.S. Li, K. Suzuki, Renewable and Sustainable Energy Reviews 13 (2009) 594–604.
[6] D. Sutton, B. Kelleher, J.R.H. Ross, Fuel Processing Technology 73 (2001) 155–173.
[7] M.P. Aznar, M.A. Caballero, J. Gil, J.A. Martin, J. Corella, Industrial and Engineering Chemistry Research 37 (1998) 2668–2680.
[8] R.C. Brown, Z. Ruiqin, W. Yanchang, Energy Conversion and Management 48 (2007) 68–77.
[9] J. Corella, A. Orio, P. Aznar, Industrial and Engineering Chemistry Research 37 (1998) 4617–4624.
[10] K.A. Magrini-Bair, S. Czernik, R. French, Y.O. Parent, E. Chornet, D.C. Dayton, C. Feik, R. Bain, Applied Catalysis A: General 318 (2007) 199–206.
[11] T. Miyazawa, T. Kimura, J. Nishikawa, S. Kado, K. Kunimori, K. Tomishige, Catalysis Today 115 (2006) 254–262.
[12] S. Rapagna, H. Provendier, C. Petit, A. Kiennemann, P.U. Foscolo, Biomass & Bioenergy 22 (2002) 377–388.
[13] L. Garcia, M.L. Salvador, J. Arauzo, R. Bilbao, Energy & Fuels 13 (1999) 851–859.
[14] J. Arauzo, D. Radlein, J. Piskorz, D.S. Scott, in: A.V. Bridgwater (Ed.), Advances in Thermochemical Biomass Conversion, Blackie Academic & Professional, London, 1994, pp. 201–215.
[15] D. Swierczynski, C. Courson, L. Bedel, A. Kiennemann, J. Guille, Chemistry of Materials 18 (2006) 4025–4032.
[16] L. Pengmei, Y. Zhenhong, W. Chuangzhi, L. Ma, C. Yong, N. Tsubaki, Energy Conversion and Management 48 (2007) 1132–1139.
[17] G. van Rossum, S.R.A. Kersten, W.P.M. van Swaaij, Industrial and Engineering Chemistry Research 46 (2007) 3959–3967.
[18] M. Virginie, J. Adanez, C. Courson, L.F. de Diego, F. Garcia-Labiano, D. Niznansky, A. Kiennemann, P. Gayan, A. Abad, Applied Catalysis B: Environmental 121 (2012) 214–222.
[19] L. Garcia, R. French, S. Czernik, E. Chornet, Applied Catalysis A: General 201 (2000) 225–239.
[20] L. Garcia, M.L. Salvador, J. Arauzo, R. Bilbao, Industrial and Engineering Chemistry Research 37 (1998) 3812–3819.
[21] L. García, M.L. Salvador, J. Arauzo, R. Bilbao, Journal of Analytical and Applied Pyrolysis 58–59 (2001) 491–501.
[22] L. Garcia, M.L. Salvador, R. Bilbao, J. Arauzo, Energy & Fuels 12 (1998) 139–143.
[23] L. Garcia, M.L. Salvador, J. Arauzo, R. Bilbao, Fuel Processing Technology 69 (2001) 157–174.
[24] G. van Rossum, S.R.A. Kersten, W.P.M. van Swaaij, Industrial and Engineering Chemistry Research 48 (2009) 5857–5866.
[25] C. Courson, E. Makaga, C. Petit, A. Kiennemann, Catalysis Today 63 (2000) 427–437.
[26] C. Courson, L. Udron, D. Swierczynski, C. Petit, A. Kiennemann, Catalysis Today 76 (2002) 75–86.
[27] D. Swierczynski, C. Courson, L. Bedel, A. Kiennemann, S. Vilminot, Chemistry of Materials 18 (2006) 897–905.
[28] J.N. Kuhn, Z. Zhao, A. Senefeld-Naber, L.G. Felix, R.B. Slimane, C.W. Choi, U.S. Ozkan, Applied Catalysis A: General 341 (2008) 43–49.
[29] J.N. Kuhn, Z.K. Zhao, L.G. Felix, R.B. Slimane, C.W. Choi, U.S. Ozkan, Applied Catalysis B: Environmental 81 (2008) 14–16.
[30] L.G. Felix, D.M. Rue, R.B. Slimane, United States patent no. 7449424, Method for Producing Catalytically-Active Materials, Gas Technology Institute, 2008.
[31] L.G. Felix, D.M. Rue, T.P. Seward III, L.E. Weast, US Patent publication no. US 2009/0011925 A1, Method for Producing Catalytically Active Glass–Ceramic Materials, and Glass–Ceramics Produced Thereby, Gas Technology Institute, USA, 2009.
[32] S. Rapagna, M. Virginie, K. Gallucci, C. Courson, M. Di Marcello, A. Kiennemann, P.U. Foscolo, Catalysis Today 176 (2011) 163–168.
[33] P.J. Dauenhauer, B.J. Dreyer, N.J. Degenstein, L.D. Schmidt, Angewandte Chemie-International Edition 46 (2007) 5864–5867.
[34] J. Corella, J.M. Toledo, G. Molina, Industrial and Engineering Chemistry Research 46 (2007) 6831–6839.
[35] J. Corella, J.M. Toledo, R. Padilla, Energy & Fuels 18 (2004) 713–720.
[36] J. Corella, M.P. Aznar, J. Gil, M.A. Caballero, Energy & Fuels 13 (1999) 1122–1127.
[37] R.J. Evans, T. Milne, in: E.J. Soltes, T.A. Milne (Eds.), Pyrolysis Oils from Biomass – Producing, Analyzing, and Upgrading, The American Chemical Society, Denver, CO, 1988, pp. 311–327.
[38] R.J. Evans, T.A. Milne, Energy & Fuels 1 (1987) 311–319.
[39] R.J. Evans, T.A. Milne, Energy & Fuels 1 (1987) 123–137.
[40] D.L. Carpenter, S.P. Deutch, R.J. French, Energy & Fuels 21 (2007) 3036–3043.
[41] K.R. Gaston, M.W. Jarvis, P. Pepiot, K.M. Smith, W.J. Frederick, M.R. Nimlos, Energy & Fuels 25 (2011) 3747–3757.
[42] Studies Involving High-Temperature Desulfurization/Regeneration Reactions of Metal Oxides for the Fuel-Cell Program, Giner, Inc., Waltham, MA, USA, 1981, 106 pp.
[43] R.J. Evans, D.N. Wang, F.A. Agblevor, H.L. Chum, S.D. Baldwin, Carbohydrate Research 281 (1996) 219–235.
[44] E.J. Shin, M.R. Nimlos, R.J. Evans, Fuel 80 (2001) 1697–1709.
[45] M.W. Jarvis, T.J. Haas, B.S. Donohoe, J.W. Daily, K.R. Gaston, W.J. Frederick, M.R. Nimlos, Energy & Fuels 25 (2011) 324–336.
[46] C. Klein, C.S. Hurlbut Jr., Manual of Mineralogy, 20th ed., John Wiley & Sons, Inc., New York, 1985.
[47] J.N. Boland, A.G. Duba, Journal of Geophysical Research-Solid Earth and Planets 91 (1986) 4711–4722.
[48] A. Dutta, M. Talmadge, J. Hensley, M. Worley, D. Dudgeon, D. Barton, P. Groenendijk, D. Ferrari, B. Stears, E. Searcy, C. Wright, J.R. Hess, Environmental Progress & Sustainable Energy 31 (2012) 182–190.
[49] L. Devi, K.J. Ptasinski, F. Janssen, Biomass & Bioenergy 24 (2003) 125–140.
[50] D.L. Carpenter, R.L. Bain, R.E. Davis, A. Dutta, C.J. Feik, K.R. Gaston, W. Jablonski, S.D. Phillips, M.R. Nimlos, Industrial and Engineering Chemistry Research 49 (2010) 1859–1871.
[51] J. Corella, J.M. Toledo, G. Molina, International Journal of Oil, Gas and Coal Technology 1 (2008) 194–207.
[52] J. Gil, J. Corella, M.P. Aznar, M.A. Caballero, Biomass and Bioenergy 17 (1999) 389–403.
[53] T. Mattisson, M. Johansson, A. Lyngfelt, Fuel 85 (2006) 736–747.
[54] B.C.H. Steele, Journal of Power Sources 49 (1994) 1–14.
[55] K. Nakamura, T. Miyazawa, T. Sakurai, T. Miyao, S. Naito, N. Begum, K. Kunimori, K. Tomishige, Applied Catalysis B: Environmental 86 (2009) 36–44.
[56] A.M. Scheer, C. Mukarakate, D.J. Robichaud, G.B. Ellison, M.R. Nimlos, Journal of Physical Chemistry A 114 (2010) 9043–9056.
[57] G. Jones, J.G. Jakobsen, S.S. Shim, J. Kleis, M.P. Andersson, J. Rossmeisl, F. Abild-Pedersen, T. Bligaard, S. Helveg, B. Hinnemann, J.R. Rostrup-Nielsen, I. Chorkendorff, J. Sehested, J.K. Norskov, Journal of Catalysis 259 (2008) 147–160.
[58] M.S. Jeong, H. Frei, Journal of Molecular Catalysis A: Chemical 156 (2000) 245–253.